

4.3 THE EGER 2007 MICROMETEOROLOGICAL EXPERIMENT IN THE FICHELGEBIRGE MOUNTAINS, GERMANY

Katharina Staudt*, Lukas Siebicke, Andrei Serafimovich, Thomas Foken
University of Bayreuth, Department of Micrometeorology, Bayreuth, Germany

R. David Pyles
University of California, Department of Land, Air and Water Resources, Davis, CA

Franz X. Meixner¹, Eva Falge
Max Planck Institute for Chemistry, Biogeochemistry Department, Mainz, Germany
¹Department of Physics, University of Zimbabwe, Harare, Zimbabwe

Cornelius Zetzsch
University of Bayreuth, Atmospheric Chemistry, Bayreuth, Germany

1. INTRODUCTION

The EGER (EXchanGE processes in mountainous Regions) project aims at the detailed quantification of relevant processes within the soil-vegetation-atmosphere system by observing diurnal and annual cycles of energy, water and trace gases. The main focus lies on the understanding of process interactions among different scales and their role for corresponding budgets. Field experiments were carried out at the Waldstein site in the Fichtelgebirge mountains (a low mountain range typical for central Europe), which are challenging for their heterogeneity and orographically structured terrain. Field observations are complemented by model simulations. Even though the EGER joint effort combines biogeochemical, chemical and micrometeorological subprojects, this work addresses the micrometeorological part only. Our contribution will present an overview of the setup of the experiment as well as first experimental and model results.

2. EXPERIMENT SETUP

Data were obtained in the period of September-October 2007 during the first intensive measuring campaign of the field experiment EGER conducted at the Waldstein site (50°08'N, 11°52'E, 775 m a.s.l.) in North-Eastern Bavaria in the Fichtelgebirge Mountains. The experiment site is described in detail in Gerstberger et al. (2004),

and a summary of background data can be found in Staudt and Foken (2007). The spruce canopy has a mean canopy height $h_c = 23$ m.

High-frequency turbulence measurements of horizontal and vertical wind components u , v , w , and sonic temperature T_s were performed using sonic anemometers (USA-1 Metek GmbH, CSAT3 Campbell Scientific, Inc., Solent R2 Gill Instruments Ltd.), and fast-response gas analyzers (LI-7000 and LI-7500, LI-COR Biosciences) for density of carbon dioxide CO_2 and water vapor H_2O . Six systems were installed on the 36-m tall, slim tower (turbulence tower, figure 1) at 0.10, 0.24, 0.56, 0.78, 1.0, 1.56- h_c levels and one system was installed at the top of the 32-m tall tower (main tower, figure 1) at 1.39- h_c level. As shown by Mauder et al. (2007) different types of sonic anemometers and sensor geometry have no significant influence on the collected data. The approximate number of available 30-min intervals varied between 1150 and 1440 for different observation heights.

Horizontal advection in the trunk space was determined by measuring wind speed and CO_2 gradients. Five 2-m towers with cup anemometers, psychrometers, and LI-840 (LI-COR Biosciences) CO_2 inlets were installed along and across the mountain slope. Three towers were additionally equipped with sonic anemometers (USA-1 Metek GmbH).

In addition to point measurements at the towers, acoustic and radioacoustic sounding measurements were performed with a remote sensing system consisting of a phase array Doppler Sodar DSDPA.90-64 with a 1290-MHz-RASS extension by Metek GmbH. The acoustic sounding system was located at a distance of approximately 250 m from the main and

*Corresponding author address:

Katharina Staudt, University of Bayreuth, Department of Micrometeorology, 95440 Bayreuth, Germany;
e-mail: katharina.staudt@uni-bayreuth.de

turbulence towers in a forest clearing. Two operating modes were used. To observe coherent structures in the vertical wind speed and temperature the sounding parameters were selected with a sufficient resolution in time (Thomas et al., 2006). The antennas were limited to the vertical and radio magnetic antennas only. The acoustic sounding frequency was chosen as 1650 Hz. The resulting mean sampling frequency of the time series was determined to be 0.4 Hz, i.e. single soundings could be performed every 2.5 s. The vertical range of measurements was from 20 m to 200 m a.g.l. The height resolution was 10 m. A 25-min interval of measurements with the settings described above was followed by profiling the atmospheric boundary layer for a period of 5 min up to an observation level of 900 m, using a vertical resolution of 20 m. This gave a mean profile of the wind vector and the acoustic temperature.



Figure 1: The 36-m turbulence tower (left) and the 32-m main tower (right) at the Waldstein site.

The measurements on the main tower are part of the FLUXNET network (site: Bayreuth-Waldstein/Weidenbrunnen). In addition to the eddy-covariance measurements on top of the tower, the measurements at the main tower supplied meteorological data for in- and above canopy profiles of wind, temperature and humidity. Radiative fluxes were measured at the top of the tower and at 2 m within the canopy. Soil measurements comprised a soil temperature profile down to 2 m, soil moisture measurements down to 0.5 m and soil heat flux measurements.

3. THE ACASA MODEL

The Advanced Canopy-Atmosphere-Soil Algorithm (ACASA) (Pyles, 2000; Pyles et al., 2000), which was developed at the University of California, Davis, is used to model the turbulent fluxes of heat, water vapor and momentum within and above the canopy. This multi-layer canopy-surface-layer model incorporates a diabatic, third-order closure method to calculate turbulent transfer within and above the canopy on the theoretical basis of the work of Meyers (1985) and Meyers and Paw U (1986, 1987). The multi-layer structure of ACASA is reflected in 20 atmospheric layers extending to twice the canopy height consisting of 10 layers within the canopy and 10 above the canopy, and 15 soil layers. Leaf, stem and soil surface temperatures are calculated using the fourth-order polynomial of Paw U and Gao (1988), allowing calculation of temperatures of these components where these may deviate significantly from ambient air temperatures. Energy flux estimates consider multiple leaf-angle classes and direct as well as diffuse radiation absorption, reflection, transmission and emission. Plant physiological response to micro-environmental conditions is calculated by a combination of the Ball-Berry stomatal conductance (Leuning, 1990; Collatz et al., 1991) and the Farquhar and von Caemmerer (1982) photosynthesis equation following Su et al. (1996). The soil module to calculate soil surface evaporation, soil moisture, and soil temperature is adapted from MAPS (Mesoscale Analysis and Prediction System; Smirnova et al., 1997, 2000). Additionally, canopy heat storage and canopy interception of precipitation are included in ACASA.

Various site-specific input parameters are needed to run ACASA. Vegetation and biophysical information is required, and half-hourly meteorological forcing quantities above the canopy and initial soil conditions are needed as upper and lower boundary conditions. Input parameters were as far as possible, derived from measured data or selected from the literature.

4. RESULTS AND DISCUSSION

In the following, preliminary results from the first EGER field experiment are shown, and therefore two fields of activity of our group were selected: the analysis of coherent structures within and above the forest and the application of the ACASA model to our site, including sensitivity analyses.

4.1 Coherent structures

As shown by Raupach (1981) and Bergström and Högström (1989) low frequency coherent events contribute significantly to the budgets of momentum, heat and matter. Our investigations are addressed to the contribution of coherent structures to the transfer of energy and matter in a forested ecosystem. To extract coherent structures from the turbulent time series, the technique based on the wavelet transform has been used (Thomas and Foken, 2005, 2007a). In a first step, outliers in high-frequency time series were removed using a despiking test (Vickers and Mahrt, 1997). Wind vector components were rotated according to the planar fit rotation method (Wilczak et al., 2001). Subsequently the scalar time series were corrected for time lags compared to the vertical wind component. Then all time series were averaged to a 2 Hz sampling resolution. In a last step, time series were passed through a low-pass wavelet filter. Finally Reynolds-averaged flux and flux contribution of coherent structures were derived using a triple decomposition for the detected and conditionally averaged time series, when coherent structures were present (Thomas and Foken, 2007b).

The mean temporal scales of coherent structures were estimated via fitting a normal Gaussian distribution function to the probability density function of the results from the individual 30-min intervals. Conditional sampling analysis shows a domination of coherent structure signatures in vertical wind measurements (Figure 2a) with probable temporal scales in the order of 20 s to 30 s and 30 s to 40 s. The number of coherent structures detected at the turbulence tower (Figure 2a) was found to be 40% less than the number of coherent structures detected at the main tower (Figure 2b). In contrast to the turbulence tower the main tower is more massive and was equipped with more instruments which is the reason for additional generation of turbulence.

Figure 3a shows the relation between Reynolds averaged flux F_{ent} and fluxes transported by coherent structures F_{CS} . One can see that momentum and sensible heat transport by coherent structures is dominant in the canopy and carbon dioxide and latent heat transport by coherent structures increases with height within the canopy and reaches a maximum at the upper canopy level. The flux contribution of the ejection phase F_{ej} and sweep phase F_{sw} of coherent exchange were determined by applying the averaging operator within the ranges $[-D_e, 0]$ and $[0, +D_e]$, where D_e is the characteristic time scale

of events occurring at frequency f and can be defined as $D_e = \frac{1}{2} \cdot f^{-1}$ (Collineau and Brunet, 1993). The flux contribution of the ejection phase decreases with increasing height within the canopy and becomes dominant above the canopy level (Figure 3b). The flux fraction transported during the downward directed sweep phase increases with height within the canopy and becomes the dominating exchange process at the upper canopy level (Figure 3c). Close to the ground surface in the subcanopy space, ejection and sweep phase contribute equally to the flux transport.

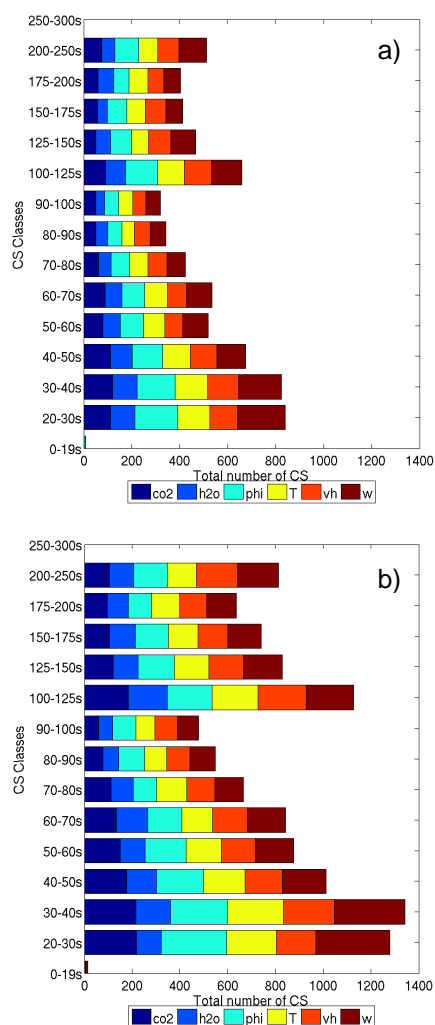


Figure 2: Total number of coherent structures detected from 14.09.2007 until 08.10.2007 in carbon dioxide CO₂, water H₂O, wind direction phi, sonic temperature T_s, horizontal velocity v_h and vertical velocity w measurements at a) the top of the turbulence tower (36 m) and b) the top of the main tower (32 m).

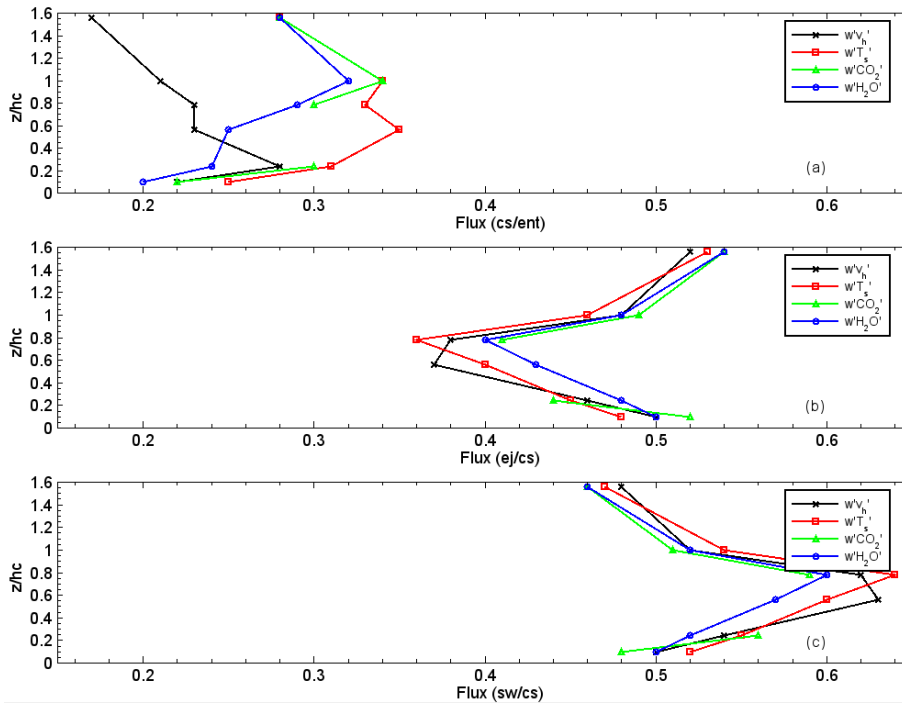


Figure 3: Flux contribution of coherent structures to the entire flux (a), of ejection (b) and sweep (c) phases to the coherent flux as a function of height h_c for the momentum ($w'v_h'$), sensible heat ($w'T_s'$), carbon dioxide ($w'CO_2'$) and latent heat ($w'H_2O'$) transport averaged from 20.09.2007 until 24.09.2007.

4.2 Model: results and sensitivity

The ACASA model was run for the days of the experiment. Half-hourly meteorological input values as well as the initial soil profiles were provided by the routine measurements at the main tower. Only small gaps in the data occurred due to power shortages, which were filled with linear interpolation methods. Site-specific input parameters such as morphological or optical properties of the forest were either derived from measurements or selected from the literature.

Comparisons of modelled fluxes with measured fluxes were done for 20 days in September and October 2007. In this study, only fluxes of the top level turbulence measurements at the turbulence tower are considered. Future work will include a more detailed study of flux profiles. Raw flux data was processed with the TK2 software package, developed at the University of Bayreuth (Mauder and Foken, 2004), including several corrections and quality tests. Quality flags after Foken et al. (2004) were calculated, which were used to filter the flux data. In addition, flux

data for rainy periods was excluded from further analyses.

Figure 5 presents a comparison of modelled and measured flux data for five fair weather days in September (20.9.2007 to 24.9.2007). These five days, in the following called “golden days”, were chosen due to the good weather conditions and the good performance of the measuring devices. Scatter plots for the complete experiment period are shown in figure 4. Modelled net radiation is in very good agreement with measured net radiation. Due to a constant underestimation of the long-wave outgoing radiation of about 15 Wm^{-2} by the model, night-time net radiation fluxes were underestimated. Energy balance closure of the model was comparable to the energy balance closure of the measurements (10% in the model, 11% in the measurements). During the whole experiment period the sensible heat flux was underestimated, whereas the latent heat flux was slightly overestimated. The ground heat flux was generally overestimated, even though the measured values have to be treated with caution. Ground heat flux measurements are single-point measurements which were, in our case, influenced

by sunspots in the late afternoon resulting in very high ground heat fluxes lasting only one hour. The model represents an area rather than a point, therefore the direct comparison of these data has to be done carefully. Day-time net ecosystem exchange (NEE) was underestimated by the model during the five golden days. The scatter plots for NEE reveal that extreme positive and negative values were underestimated.

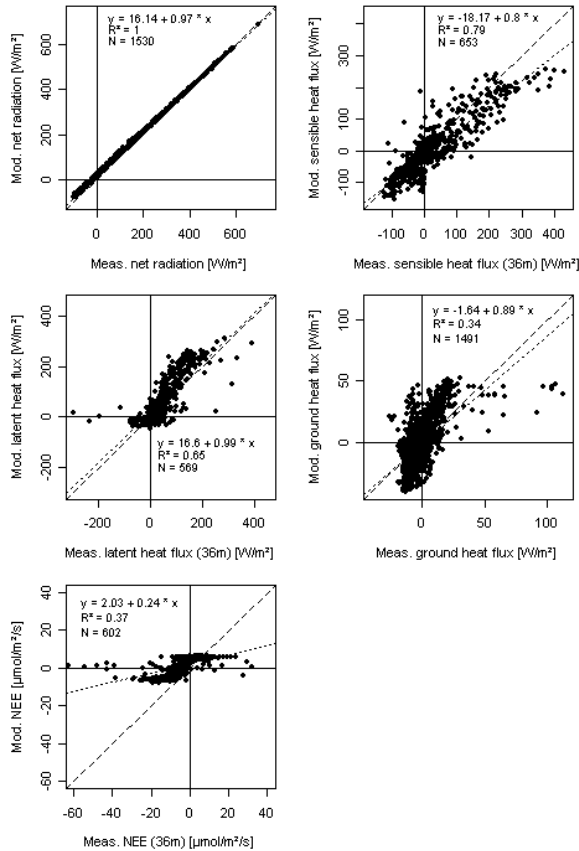


Figure 4: Scatter plots of measured and modelled values of net radiation, sensible, latent, and ground heat flux, and NEE for the whole duration of the experiment.

To analyse the sensitivity of the model to the external input parameters, sensitivity analyses were performed for the five fair weather days. So far, only 19 external input parameters, read in from a text file, have been considered (see table 1; parameters for microbial and root soil respiration were set to equal values). The Bayesian Generalized Likelihood Uncertainty Estimation (GLUE) method, which was developed by Beven and Binley (1992) and since then has been used in several model sensitivity analysis studies (e.g. Franks et al., 1997; Liebenthal et al., 2005; Prihodko et al., 2008), was employed here. For all

19 analysed parameters, parameter ranges were defined that cover a realistic range of values for the Waldstein site. All parameter ranges were assigned a uniform distribution and random sets of parameters were produced for a large number of model runs (12600). From the model outputs and the measured data, likelihood measures were calculated to assess the performance of each model run. In this study, as a single-objective goodness of fit criteria for turbulent and radiative fluxes and the NEE, the coefficient of determination L :

$$L = 1 - \frac{\sigma_d^2}{\sigma_o^2} \quad (1)$$

was calculated, where σ_o^2 denotes the variance of the observations and σ_d^2 denotes the variance of the differences between measured and simulated data. The coefficient of determination, L , ranges from minus infinity to 1, whereas values close to 1 indicate a good agreement of modelled and measured data.

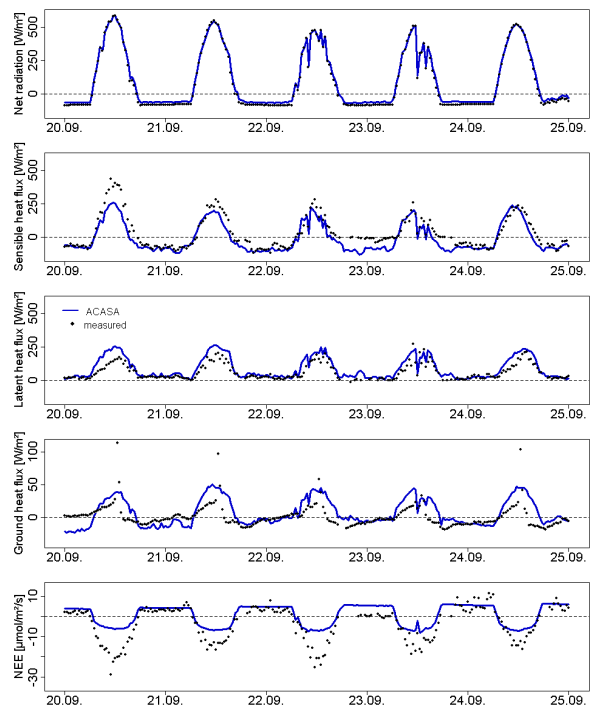


Figure 5: Time series from 20.09.2007 until 24.09.2007 for net radiation, sensible, latent, and ground heat flux, and NEE showing modelled (solid line) and measured values (dotted).

Table 1: List of the external input parameters to the ACASA model which were studied in the sensitivity analyses, with values used for the reference calculations and the range within which each parameter was varied.

| Parameter | Definition | Min. | Max. | Reference |
|-----------|--|------|------|-----------|
| xlai | LAI (single-sided) (-) | 0.5 | 5.0 | 2.6 |
| standage | canopy height (m) | 18 | 28 | 23 |
| isoi3 | soil type (USDA textural classes of soil) | 1 | 14 | 3 |
| zmoi | wilting point soil moisture (-) | 0.1 | 0.4 | 0.2 |
| r0l | leaf basal respiration rate ($\mu\text{mol m}^{-2}(\text{leaves}) \text{s}^{-1}$) | 0.05 | 1.7 | 0.13 |
| r0s | stem basal respiration rate ($\mu\text{mol m}^{-2}(\text{stems}) \text{s}^{-1}$) | 0.05 | 1.7 | 0.13 |
| r0r | root basal respiration rate ($\mu\text{mol m}^{-2}(\text{roots}) \text{s}^{-1}$) | 0.05 | 1.7 | 0.13 |
| r0m | microbe basal respiration rate ($\mu\text{mol m}^{-2}(\text{microbes}) \text{s}^{-1}$) | 0.05 | 1.7 | 0.13 |
| q10l | q10 for leaves (-) | 1.8 | 3.0 | 2.46 |
| q10s | q10 for stems (-) | 1.8 | 3.0 | 2.0 |
| q10r | q10 for roots (-) | 1.8 | 3.0 | 2.42 |
| q10m | q10 for microbes (-) | 1.8 | 3.0 | 2.42 |
| pr0 | near-IR leaf reflectivity (-) | 0.2 | 0.4 | 0.28 |
| tr0 | near-IR leaf transmissivity (-) | 0.05 | 0.2 | 0.07 |
| pv0 | visible leaf reflectivity (-) | 0.01 | 0.15 | 0.07 |
| tv0 | visible leaf transmissivity (-) | 0.01 | 0.15 | 0.03 |
| xremp | optimal photosynthetic temperature ($^{\circ}\text{C}$) | 10 | 30 | 20 |
| drx | leaf drag coefficient (-) | 0.05 | 0.6 | 0.2 |
| xldiam | mean leaf diameter (m) | 0.01 | 0.02 | 0.015 |
| xrsmn | maximum carboxylation rate ($\mu\text{mol m}^{-2} \text{s}^{-1}$) | 10 | 80 | 35 |
| wue | water use efficiency factor (-) | 0.3 | 2.0 | 1.0 |

A multi-objective goodness of fit criteria was calculated to combine several fluxes following Franks et al. (1999):

$$L = \left(\left(\frac{\mathbf{s}_a^2}{\hat{\mathbf{s}}_a^2} \right) \cdot \left(\frac{\mathbf{s}_b^2}{\hat{\mathbf{s}}_b^2} \right) \cdot \dots \right)^{-N} \quad (2)$$

where σ^2_{α} is the variance of the differences between measured and simulated data and $\hat{\mathbf{s}}_a^2$ is the minimum of the variance of the differences between measured and simulated data for a particular variable. The scaling factor N is set to negative one in this paper, which means that the likelihood values were not rescaled. These combined likelihood values L range from one to plus infinity, with values close to 1 indicating the least amount of error in predicted versus observed fluxes.

Figure 6 shows the resulting sensitivity graphs of the single-objective goodness of fit analyses, where the coefficient of determination for the fluxes for the 12600 model runs are plotted versus two input parameters (LAI, leaf diameter). For the multi-objective goodness of fit criteria, only the sensible and latent heat fluxes and the NEE were considered due to the very low values of the coefficient of determination for the ground heat

flux. Figure 7 shows the combined goodness of fit criteria versus the LAI and the leaf diameter.

The maximum values as well as the range of the coefficient of determination (figure 6) are very different for the five fluxes considered here. Only for net radiation are values close to 1 reached, which shows, in combination with a small variability of L (minimum of 0.98), a very good agreement of observed and modelled values. The maximum value for the sensible heat flux is 0.9, whereas the lowest values are around 0.4. For the latent heat flux and NEE, the variability is much wider. Maximum values of L for these two fluxes are around 0.85, whereas L goes down to negative values, reaching -1.8 and -5.1 , respectively. Coefficients of determination for the ground heat flux scatter in a wide range as well, but in general reach only very low values, with maxima around 0.2.

In the following, the sensitivity of the model to two morphological parameters (leaf area index, leaf diameter) is discussed in more detail. These parameters are chosen as examples, as the LAI seems to be one of the parameters which is most sensitive to changes in its value and the leaf diameter belongs to the parameters that are the least sensitive.

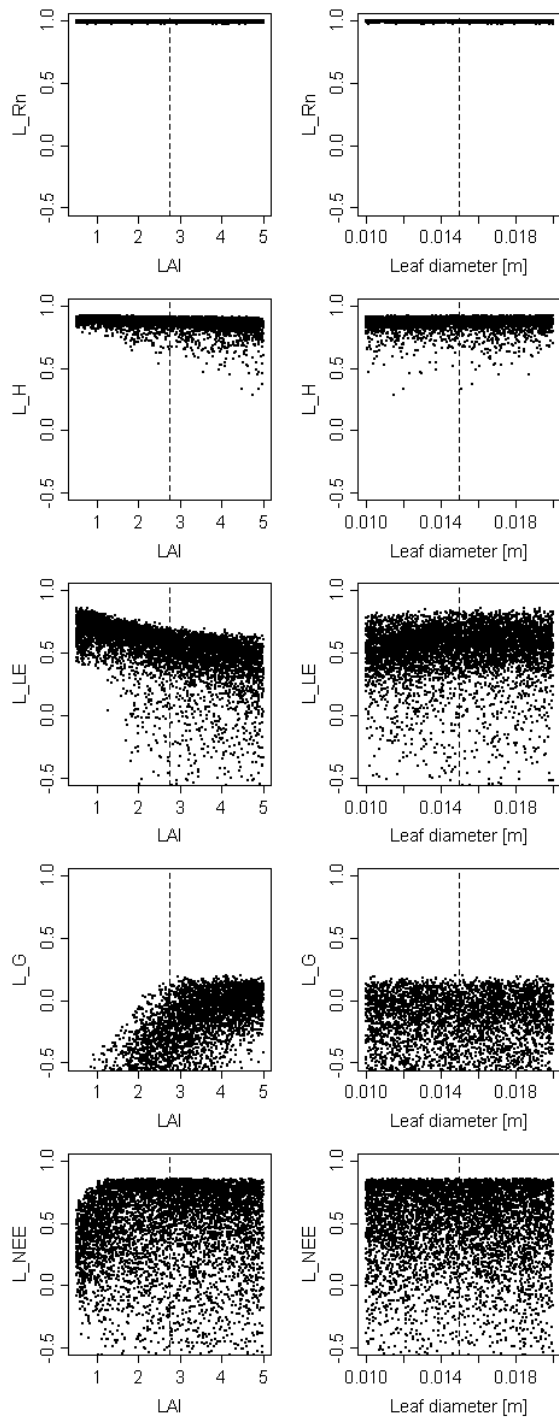


Figure 6: Sensitivity graphs showing the range of the coefficient of determination for net radiation, sensible, latent, and ground heat flux and NEE across the range of the leaf area index (left side) and the leaf diameter (right side). The vertical line denotes the parameter value used for the model runs shown before. (N = 204, 12600 runs)

For the leaf diameter, over the whole parameter range for all studied fluxes, very good as well as very poor results are obtained, indicating less sensitivity and a tendency towards equifinality. In contrast, the patterns in the scatter plots for the LAI allow the sensitivity of this parameter to each of the fluxes to be evaluated. For the sensible and the latent heat fluxes, higher coefficients of determination as well as smaller variabilities of the coefficient of determination are achieved for lower LAI values. In contrast, lower LAI values result in lower coefficients of determination for the NEE and the ground heat flux. The plot for the multi-objective goodness of fit criterion versus LAI (figure 7) shows a peak at a LAI value of about 1.5, whereas the plot for the leaf diameter shows again no clear pattern of sensitivity.

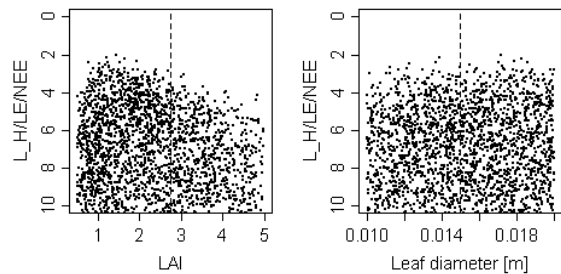


Figure 7: Combined sensitivity graphs showing the values of the likelihood function developed by Franks (1998) across the range of the leaf area index (left side) and the leaf diameter (right side). The vertical line denotes the parameter value used for the model runs shown before. (N = 204, 12600 runs)

As was found in several studies examining the sensitivity of parameters in complex models (e.g. Franks et al., 1997; Schulz et al., 2001; Prihodko et al., 2008), the problem of parameter equifinality is seen in ACASA as well. Within this limited study, four parameters could be identified as being dominant parameters for the turbulent fluxes, namely leaf area index, maximum carboxylation rate, water use efficiency factor and drag coefficient. Additionally, for the NEE, the parameters determining leaf respiration are dominant parameters. For all other parameters, very good as well as very poor results were obtained over the whole parameter ranges. Of course this study covers only five fair weather days in autumn, which does not include a wide range of meteorological variability in terms of, for example air temperature and soil moisture. Furthermore, the results of these sensitivity analyses only hold true for the Waldstein site.

5. CONCLUSIONS

In this paper, first results from the first field experiment of the EGER project in the Fichtelgebirge Mountains, Germany, were presented.

It was shown that towers and instruments on towers can increase turbulent flows up to 40%. The momentum, sensible heat, carbon dioxide, and latent heat transport by coherent structures is higher in middle and upper canopy level. In the trunk space of the forest, ejection and sweep phases of coherent structures contribute equally to the flux transport. From other side flux transport by ejection phases prevails above the canopy and by sweep phases inside the canopy.

First modelling studies showed a reasonable agreement of sensible and latent heat fluxes. A sensitivity analysis for a limited time period demonstrated the equifinality of many external parameters in the ACASA model, similarly to other complex process-based models. The resulting fluxes seemed to be sensitive to only a few of the external parameters. So far, none of the internal parameters, e.g. in the photosynthesis submodel, have been included in the sensitivity analysis. Variation of these parameters might improve the simulated fluxes, but could also enhance the problem of equifinality due to the increasing number of parameters. Due to the limited significance of the sensitivity analysis because of its short time period and because only one site was tested, further studies should include other time periods with different weather conditions and might also include other sites to be able to make more general statements about the overall model performance and sensitivity to its input parameters.

The EGER data and the model results will be studied in more detail in future, with emphasis on the turbulence structure within the forest. In summer 2008 the second observation period will be carried out at the Waldstein site. The improved experiment design will be used to investigate vertical coherent exchange in the canopy in connection with horizontal advection processes in the subcanopy space.

6. ACKNOWLEDGEMENTS

The authors wish to acknowledge the help and technical support performed by the staff of the Bayreuth Center for Ecology and Environmental Research (BayCEER) of the University of Bayreuth. The project is funded by the German

Science Foundation (FO 226/16-1, ME2100/4-1, ZE 792/4-1).

7. REFERENCES

- Bergström, H. and U. Högström, 1989: Turbulent exchange above a pine forest. II. Organized structures. *Boundary-Layer Meteorology*, **49**, 231-263.
- Beven, K. J. and A. M. Binley, 1992: The future of distributed models: model calibration and uncertainty prediction. *Hydrological Processes*, **6**, 279-298.
- Collatz, G. J., J. T. Ball, C. Grivet, and J. A. Berry, 1991: Physiological and environmental regulation of stomatal conductance, photosynthesis and transpiration: a model that includes a laminar boundary layer. *Agricultural and Forest Meteorology*, **54**, 107-136.
- Collineau, S. and Y. Brunet, 1993: Detection of turbulent coherent motions in a forest canopy. Part I: Wavelet analysis. *Boundary-Layer Meteorology*, **65**, 357-379.
- Farquhar, G. D. and S. von Caemmerer, 1982: Modelling of photosynthetic response to environmental conditions. *Physiological Plant Ecology II, Water Relations and Carbon Assimilation*, O. L. Lange, P. S. Nobel, C. B. Osmond, and H. Ziegler, Eds., Springer, 549-588.
- Foken, T., M. Göckede, M. Mauder, L. Mahrt, B. D. Amiro, and J. W. Munger, 2004: Post-field data quality control. *Handbook of Micrometeorology: A Guide for Surface Flux Measurements*, X. Lee, W. Massman, and B. Law, Eds., Kluwer, 81-108.
- Franks, S. W., K. J. Beven, and J. H. C. Gash, 1999: Multi-objective conditioning of a simple SVAT model. *Hydrology and Earth System Sciences*, **3**, 477-489.
- Franks, S. W., K. J. Beven, P. F. Quinn, and I. R. Wright, 1997: On the sensitivity of soil-vegetation-atmosphere transfer (SVAT) schemes: equifinality and the problem of robust calibration. *Agricultural and Forest Meteorology*, **86**, 63-75.
- Gerstberger, P., T. Foken, and K. Kalbitz, 2004: The Lehstenbach and Steinkreuz Catchments in NE Bavaria, Germany. *Biogeochemistry of Forested Catchments in a Changing Environment: A German Case Study*, E. Matzner, Ed., Springer, 15-44.
- Leuning, R., 1990: Modelling stomatal behaviour and photosynthesis of *Eucalyptus grandis*. *Australian Journal of Plant Physiology*, **17**, 159-175.

- Liebenthal, C., B. Huwe, and T. Foken, 2005: Sensitivity analysis for two ground heat flux calculation approaches. *Agricultural and Forest Meteorology*, **132**, 253-262.
- Mauder, M. and T. Foken, 2004: Documentation and instruction manual of the eddy covariance software package TK2. *Work Report University of Bayreuth, Dept. of Micrometeorology*, 26, 44 pp., ISSN 1614-8916.
- Mauder, M., S. P. Oncley, R. Vogt, T. Weidinger, L. Ribeiro, C. Bernhofer, T. Foken, W. Kohsiek, H. A. R. De Bruin, and H. Liu, 2007: The energy balance experiment EBEX-2000. Part II: Intercomparison of eddy-covariance sensors and post-field data processing methods. *Boundary-Layer Meteorology*, **123**, 29-54.
- Meyers, T. P., 1985: A simulation of the canopy microenvironment using higher order closure principles. PhD thesis, Purdue University, 153 pp.
- Meyers, T. P. and K. T. Paw U, 1986: Testing of a higher-order closure model for airflow within and above plant canopies. *Boundary-Layer Meteorology*, **37**, 297-311.
- , 1987: Modelling the plant canopy micrometeorology with higher-order closure techniques. *Agricultural and Forest Meteorology*, **41**, 143-163.
- Paw U, K. T. and W. Gao, 1988: Applications of solutions to non-linear energy budget equations. *Agricultural and Forest Meteorology*, **43**, 121-145.
- Prihodko, L., A. S. Denning, N. P. Hanan, I. Baker, and K. Davis, 2008: Sensitivity, uncertainty and time dependence of parameters in a complex land surface model. *Agricultural and Forest Meteorology*, **148**, 268-287.
- Pyles, R. D., 2000: The development and testing of the UCD advanced canopy-atmosphere-soil algorithm (ACASA) for use in climate prediction and field studies. PhD thesis, University of California, Davis, 194 pp.
- Pyles, R. D., B. C. Weare, and K. T. Paw U, 2000: The UCD Advanced Canopy-Atmosphere-Soil Algorithm: comparisons with observations from different climate and vegetation regimes. *Quarterly Journal of the Royal Meteorological Society*, **126**, 2951-2980.
- Raupach, M.R., 1981: Conditional statistics of Reynolds stress in rough-wall and smooth-wall turbulent boundary layers. *Journal of Fluid Mechanics*, **108**, 363-382.
- Schulz, K., A. Jarvis, K. Beven, H. Soegaard, 2001: The predictive uncertainty of land surface fluxes in response to increasing ambient carbon dioxide. *Journal of Climate*, **14**, 2551-2562.
- Smirnova, T. G., J. M. Brown, and S. G. Benjamin, 1997: Performance of Different Soil Model Configurations in Simulating Ground Surface Temperature and Surface Fluxes. *Monthly Weather Review*, **125**, 1870-1884.
- Smirnova, T. G., J. M. Brown, S. G. Benjamin, and D. Kim, 2000: Parameterization of cold-season processes in the MAPS land-surface scheme. *Journal of Geophysical Research-Atmospheres*, **105**, 4077-4086.
- Staudt, K. and T. Foken, 2007: Documentation of reference data for the experimental areas of the Bayreuth Centre for Ecology and Environmental Research (BayCEER) at the Waldstein site. *Work Report University of Bayreuth, Dept. of Micrometeorology*, 35, 37 pp., ISSN 1614-8916.
- Su, H.-B., K. T. Paw U, and R. H. Shaw, 1996: Development of a coupled leaf and canopy model for the simulation of plant-atmosphere interactions. *Journal of Applied Meteorology*, **35**, 733-748.
- Thomas, C. and T. Foken, 2005: Detection of long-term coherent exchange over spruce forest using wavelet analysis. *Theoretical and Applied Climatology*, **80**, 91-104.
- , 2007a: Organised motion in a tall spruce canopy: temporal scales, structure spacing and terrain effects. *Boundary-Layer Meteorology*, **122**, 123-147.
- , 2007b: Flux contribution of coherent structures and its implications for the exchange of energy and matter in a tall spruce canopy. *Boundary-Layer Meteorology*, **123**, 317-337.
- Thomas, C., J. C. Mayer, F. X. Meixner, and T. Foken, 2006: Analysis of low-frequency turbulence above tall vegetation using a Doppler sodar. *Boundary-Layer Meteorology*, **119**, 563-587.
- Vickers, D. and L. Mahrt, 1997: Quality control and flux sampling problems for tower and aircraft data. *Journal of Atmospheric and Oceanic Technology*, **14**, 512-526.
- Wilczak, J. M., S. P. Oncley, and S. A. Stage, 2001: Sonic anemometer tilt correction algorithms. *Boundary-Layer Meteorology*, **99**, 127-150.